APPLICATION OF FINITE VARIATIONS TO TOPOLOGY AND SHAPE OPTIMIZATION OF 2D STRUCTURES

Dariusz Bojczuk

Faculty of Management and Computer Modelling, Kielce University of Technology
e-mail: mecdb@eden.tu.kielce.pl

Wojciech Szteleblak

PhD student; e–mail: szteleblak@go2.pl

The method of simultaneous topology and shape optimization of 2D structures by finite topology modification is presented in the paper. Both, structures in a plane state of stress and bending Kirchhoff's plates are analyzed here. Conditions for the introduction of finite topology modification based on the topological derivative are specified. When the respective condition is satisfied, finite holes and finite variations of existing boundaries are introduced into the structure. Next, standard shape optimization of new holes and variable boundaries is performed. Two basic types of modification are considered here, namely the introduction of holes of a prescribed size and shape and the introduction of holes of an unknown size and shape together with the introduction of finite changes of other boundaries. A heuristic algorithm for optimal design of topology and shape is proposed in the paper. Illustrative examples confirm applicability of the proposed approach.

Key words: 2D structures, optimal topology and shape, topological derivative, finite modification, structure evolution

1. Introduction

The optimal structural design is usually concerned with the specification of dimensional parameters, shape (or configuration) parameters and topology of a structure. For 2D structures, the coupled topology and shape optimization problem can be stated as optimal determination of external boundaries and holes within a given domain. Now, at first we can introduce infinitesimally

small voids (so called "bubbles") into the structure of the optimal shape. The position of the void, in the case of minimization of the strain energy functional, is determined by applying the bubble method (Eschenauer *et al.*, 1994), and in the case of an arbitrary objective functional, using the topological derivative approach. For plane elasticity, this problem was studied by Sokołowski and Żochowski (1999), Burczyński (2002), Burczyński and Kokot (2005).

In the present paper, the approach by topological derivative is extended for finite topology modifications. Now, instead inserting of infinitesimally small voids, the modification corresponds to introduction of holes of finite dimensions and introduction of finite variations of existing boundaries (cf. Mróz and Bojczuk, 2003). Next, the boundaries of new holes are described by some additional shape parameters, and standard shape optimization of variable external boundaries and holes is performed.

When the approach by finite topology modification is used, usually the number of iterations during the optimization process is considerably reduced. Here, this approach is applied to plane elasticity problems and for plate problems. In the case of plates, former methods are usually based on the optimization of thickness distribution (cf. Marczewska *et al.*, 2003), or on determination of optimal distribution of two materials: weaker and stronger (cf. Czarnecki *et al.*, 2004). So, the approach presented here differs essentially from them and develops a new methodology of optimal design.

2. Topological derivative for 2D structures

2.1. Topological derivative for plane elasticity problems

The concept of the topological derivative for strain energy was analyzed by Eschenauer *et al.* (1994). Next, it was generalized for arbitrary displacement and stress functionals by Sokołowski and Żochowski (1999).

Let $\Omega \subset R^2$ be a domain occupied by an elastic body with a boundary $\Gamma = \Gamma_u \cup \Gamma_T$. The body is subjected to the surface traction $\boldsymbol{T}^0$ on Γ_T and volume forces $\boldsymbol{p}^0$ in Ω. On the boundary Γ_u, displacements $\boldsymbol{u}^0$ are given. The topological derivative is defined as follows

$$\Im_G^D(\boldsymbol{x}) = \lim_{\rho \to 0} \frac{G(\Omega - \overline{B}_\rho(\boldsymbol{x})) - G(\Omega)}{\pi \rho^2} \qquad \boldsymbol{x} \in \Omega \qquad (2.1)$$

where G is the analyzed functional and $\overline{B}_\rho(\boldsymbol{x})$ is a circular hole of the radius ρ, so $\overline{B}_\rho(\boldsymbol{x}) = \{\boldsymbol{y} \in R^2 : |\boldsymbol{y} - \boldsymbol{x}| \leqslant \rho\}$. Moreover, the superscript D denotes the topological derivative for plane elasticity problems (disks).

The topological derivative provides information about infinitesimally small variation of the functional G if a small hole is inserted into the structure at the point $\boldsymbol{x}$. It means that the topological derivative can be used for topology and shape optimization of structures. To calculate the topological derivative, an adjoint method is used. In this method, a new structure of the same shape and material constants as the primary structure but with different boundary conditions and loads, is introduced.

Consider for a disk of a unit thickness a functional of strains and displacements in the form

$$G = \int_{\Omega} F(\boldsymbol{\varepsilon}) \, d\Omega + \int_{\Omega} f(\boldsymbol{u}) \, d\Omega \tag{2.2}$$

where F is a function of strains $\boldsymbol{\varepsilon} = [\varepsilon_{11}, \varepsilon_{22}, \gamma_{12}]^{\top}$ (here $\gamma_{12} = 2\varepsilon_{12}$) and f denotes a function of displacements $\boldsymbol{u}$. Its variation with respect to insertion of a hole of an infinitesimally small radius ρ at the point $\boldsymbol{x}$, can be written as follows

$$\delta G = \int_{\Omega} \frac{\partial F}{\partial \boldsymbol{\varepsilon}} \delta \boldsymbol{\varepsilon} \, d\Omega + \int_{\Omega} \frac{\partial f}{\partial \boldsymbol{u}} \delta \boldsymbol{u} \, d\Omega + \sum_{k=1}^{2} \int_{\Gamma_{\rho}} (F + f) n_k \delta \varphi_k \, d\Gamma_{\rho} \tag{2.3}$$

where $\boldsymbol{n} = [n_1, n_2]^{\top}$ is the vector normal to the boundary Γ_{ρ} of the hole and $\delta \boldsymbol{\varphi} = [\delta \varphi_1, \delta \varphi_2]^{\top}$ denotes the function of shape transformation of the hole.

Consider now an adjoint structure of the same shape as the primary structure, but subjected to initial stresses $\boldsymbol{\sigma}^{ai}$ and volume forces $\boldsymbol{p}^{a0}$, namely

$$\boldsymbol{\sigma}^{ai} = \frac{\partial F}{\partial \boldsymbol{\varepsilon}} \qquad \boldsymbol{p}^{a0} = \frac{\partial f}{\partial \boldsymbol{u}} \qquad \text{in } \Omega \tag{2.4}$$

The boundary conditions are assumed as follows

$$\boldsymbol{T}^{a0} = \boldsymbol{0} \quad \text{on } \Gamma_T \qquad \boldsymbol{u}^{a0} = \boldsymbol{0} \quad \text{on } \Gamma_u \tag{2.5}$$

where $\boldsymbol{T}^{a0}$ is the surface traction and $\boldsymbol{u}^{a0}$ is the vector of displacements. The field of initial stresses induces a field of global stresses $\boldsymbol{\sigma}^a = [\sigma_{11}^a, \sigma_{22}^a, \sigma_{12}^a]^{\top}$ in the form

$$\boldsymbol{\sigma}^a = \boldsymbol{\sigma}^{ai} + \boldsymbol{\sigma}^{ar} \tag{2.6}$$

where $\boldsymbol{\sigma}^{ar}$ is the field of the elastic stresses. Now, taking into account (2.4), (2.5) and the relationship $\sum_{k=1}^{2} n_k \delta \varphi_k = -\delta \rho$, equation (2.3) becomes

$$\delta G = \int_{\Omega} \boldsymbol{\sigma}^{ai} \delta \boldsymbol{\varepsilon} \, d\Omega + \int_{\Omega} \boldsymbol{p}^{a0} \delta \boldsymbol{u} \, d\Omega - \int_{\Gamma_{\rho}} (F + f) \, d\Gamma_{\rho} \delta \rho \tag{2.7}$$

So, in view of the virtual work equation

$$\int_\Omega \boldsymbol{\sigma}^{ar}\delta\boldsymbol{\varepsilon}\ d\Omega = \int_\Omega \boldsymbol{p}^{a0}\delta\boldsymbol{u}\ d\Omega \tag{2.8}$$

the complementary virtual work equation

$$\int_\Omega \boldsymbol{\sigma}^{a}\delta\boldsymbol{\varepsilon}\ d\Omega = \int_\Omega \boldsymbol{\varepsilon}^{a}\delta\boldsymbol{\sigma}\ d\Omega = \int_{\Gamma_\rho} \boldsymbol{\sigma}\boldsymbol{\varepsilon}^{a}\ d\Gamma_\rho\delta\rho - \int_{\Gamma_\rho} \boldsymbol{p}^{0}\boldsymbol{u}^{a}\ d\Gamma_\rho\delta\rho \tag{2.9}$$

and equation (2.6), the first variation of the functional G takes the form

$$\delta G = \int_{\Gamma_\rho} (\boldsymbol{\sigma}\boldsymbol{\varepsilon}^{a} - F - f - \boldsymbol{p}^{0}\boldsymbol{u}^{a})\ d\Gamma_\rho\delta\rho \tag{2.10}$$

Now, adapting this sensitivity formula to the case of a disk with an arbitrary thickness h, and assuming that the function f and external load $\boldsymbol{p}^{0}$ are referred directly to this thickness, equation (2.10) can be rewritten as follows

$$\delta G = \int_0^{2\pi} [(\boldsymbol{\sigma}\boldsymbol{\varepsilon}^{a} - F)h - f - \boldsymbol{p}^{0}\boldsymbol{u}^{a}]\rho\ d\theta\delta\rho \tag{2.11}$$

As for the considered case $\delta G = (\partial G/\partial\rho)\delta\rho$, it is important to notice that if $\rho \to 0$, then $\partial G/\partial\rho \to 0$. Therefore, let us compute the second derivative at the point $\boldsymbol{x}$ for $\rho = 0$. Now, we have

$$\frac{\partial^2 G}{\partial\rho^2}\bigg|_{\rho=0} = \lim_{\rho\to 0}\int_0^{2\pi}\bigg\{\frac{\partial}{\partial\rho}[(\boldsymbol{\sigma}\boldsymbol{\varepsilon}^{a} - F)h - f - \boldsymbol{p}^{0}\boldsymbol{u}^{a}] +$$

$$\tag{2.12}$$

$$-\frac{\partial}{\partial\boldsymbol{n}}[(\boldsymbol{\sigma}\boldsymbol{\varepsilon}^{a} - F)h - f - \boldsymbol{p}^{0}\boldsymbol{u}^{a}] + \frac{1}{\rho}[(\boldsymbol{\sigma}\boldsymbol{\varepsilon}^{a} - F)h - f - \boldsymbol{p}^{0}\boldsymbol{u}^{a}]\bigg\}\rho\ d\theta$$

On the boundary of the hole, in the polar coordinates r, θ with the origin in its center, we have: $\sigma_{rr} = 0$, $\sigma_{r\theta} = 0$, $\sigma_{rr}^{a} = 0$, $\sigma_{r\theta}^{a} = 0$. So, only hoop stresses $\sigma_{\theta\theta}$, $\sigma_{\theta\theta}^{a}$ may attain non-zero values on this boundary. They can be expressed as follows (cf. Sokołowski and Żochowski, 1999)

$$\sigma_{\theta\theta} = (\sigma_1 + \sigma_2) - 2(\sigma_1 - \sigma_2)\cos 2\theta$$

$$\tag{2.13}$$

$$\sigma_{\theta\theta}^{a} = (\sigma_1^{a} + \sigma_2^{a}) - 2(\sigma_1^{a} - \sigma_2^{a})\cos 2(\theta - \alpha)$$

where σ_1, σ_2, σ_1^a, σ_2^a are the principal stresses in the considered point, respectively for the primary and adjoint structure, and α is the angle between corresponding principal directions. Taking into account that $\varepsilon_{\theta\theta}^a = \sigma_{\theta\theta}^a/E$ and $\partial/\partial \boldsymbol{n} = -(\partial/\partial r)|_{r=\rho}$, relation (2.12) becomes

$$
\begin{aligned}
\frac{\partial^2 G}{\partial \rho^2}\Big|_{\rho=0} = \lim_{\rho \to 0} \int_0^{2\pi} \Big\{ & \frac{\partial}{\partial \rho}\Big[\Big(\frac{1}{E}\sigma_{\theta\theta}\sigma_{\theta\theta}^a - F\Big)h - f - \boldsymbol{p}^0\boldsymbol{u}^a\Big] + \\
& +\frac{\partial}{\partial r}\Big[\Big(\frac{1}{E}\sigma_{\theta\theta}\sigma_{\theta\theta}^a - F\Big)h - f - \boldsymbol{p}^0\boldsymbol{u}^a\Big]\Big|_{r=\rho} + \\
& +\frac{1}{\rho}\Big[\Big(\frac{1}{E}\sigma_{\theta\theta}\sigma_{\theta\theta}^a - F\Big)h - f - \boldsymbol{p}^0\boldsymbol{u}^a\Big]\Big\}\rho\, d\theta
\end{aligned}
\tag{2.14}
$$

where E is Young's modulus.

In the structure with the hole of the radius ρ, for displacements expressed in the polar coordinates r ($r \geqslant \rho$) and θ, the following expansion in the point $\rho = 0$ holds (cf. Il'in, 1992; Sokołowski and Żochowski, 1999)

$$
\begin{aligned}
u_r(r,\theta) = u_{r0} + & \frac{\sigma_1+\sigma_2}{4Gr}\Big(\frac{1-\nu}{1+\nu}r^2 + \rho^2\Big) + \\
& +\frac{\sigma_1-\sigma_2}{4Gr}\Big(r^2 + \frac{4}{1+\nu}\rho^2 - \frac{\rho^4}{r^2}\Big)\cos 2\theta + \ldots \\
u_\theta(r,\theta) = u_{\theta 0} - & \frac{\sigma_1-\sigma_2}{4Gr}\Big(r^2 + 2\frac{1-\nu}{1+\nu}\rho^2 + \frac{\rho^4}{r^2}\Big)\sin 2\theta + \ldots
\end{aligned}
\tag{2.15}
$$

where ν is Poisson's ratio, $G = E/[2(1+\nu)]$ and u_{r0}, $u_{\theta 0}$ are displacement components of the unmodified structure at the point $\boldsymbol{x}$. Next, using geometrical relations

$$
\varepsilon_{rr} = \frac{\partial u_r}{\partial r} \qquad\qquad \gamma_{r\theta} = \frac{1}{r}\frac{\partial u_r}{\partial \theta} + \frac{\partial u_\theta}{\partial r} - \frac{u_\theta}{r}
$$

$$
\varepsilon_{\theta\theta} = \frac{u_r}{r} + \frac{1}{r}\frac{\partial u_\theta}{\partial \theta}
\tag{2.16}
$$

and Hooke's law

$$
\sigma_{rr} = \frac{E}{1-\nu^2}(\varepsilon_{rr} + \nu\varepsilon_{\theta\theta}) \qquad\qquad \tau_{r\theta} = G\gamma_{r\theta}
$$

$$
\sigma_{\theta\theta} = \frac{E}{1-\nu^2}(\varepsilon_{\theta\theta} + \nu\varepsilon_{rr})
\tag{2.17}
$$

in the polar coordinates, the stresses can be expressed in the form

$$\sigma_{rr}(r,\theta) = \frac{1}{2}(\sigma_1 + \sigma_2)\left(1 - \frac{\rho^2}{r^2}\right) + \frac{1}{2}(\sigma_1 - \sigma_2)\left(1 - 4\frac{\rho^2}{r^2} + 3\frac{\rho^4}{r^4}\right)\cos 2\theta + \ldots$$

$$\sigma_{\theta\theta}(r,\theta) = \frac{1}{2}(\sigma_1 + \sigma_2)\left(1 + \frac{\rho^2}{r^2}\right) + \frac{1}{2}(\sigma_1 - \sigma_2)\left(1 + 3\frac{\rho^4}{r^4}\right)\cos 2\theta + \ldots \quad (2.18)$$

$$\tau_{r\theta}(r,\theta) = -\frac{1}{2}(\sigma_1 - \sigma_2)\left(1 + 2\frac{\rho^2}{r^2} - 3\frac{\rho^4}{r^4}\right)\sin 2\theta + \ldots$$

Analogous relations can be also obtained for the adjoint structure. After substitution of expansions of the stresses $\sigma_{\theta\theta}$, $\sigma_{\theta\theta}^a$ into (2.14), it can be easily proven that the sum of two first terms on the right-hand side of this equation cancels out. Now, (2.14) can be rewritten in the form

$$\frac{\partial^2 G}{\partial \rho^2}\Big|_{\rho=0} = \int_0^{2\pi}\left[\left(\frac{1}{E}\sigma_{\theta\theta}\sigma_{\theta\theta}^a - F\right)h - f - \boldsymbol{p}^0\boldsymbol{u}^a\right]d\theta \quad (2.19)$$

Then, taking into account (2.13) and integrating with respect to θ, the topological derivative at the point $\boldsymbol{x}$, which is expressed in the form

$$\Im_G^D(\boldsymbol{x}) = \frac{1}{2\pi}\frac{\partial^2 G}{\partial \rho^2}\Big|_{\rho=0} \quad (2.20)$$

finally, can be written as follows

$$\Im_G^D(\boldsymbol{x}) = h\left[\frac{1}{E}(\sigma_1 + \sigma_2)(\sigma_1^a + \sigma_2^a) + \frac{2}{E}(\sigma_1 - \sigma_2)(\sigma_1^a - \sigma_2^a)\cos 2\alpha - F_0\right] - f - \boldsymbol{p}^0\boldsymbol{u}^a \quad (2.21)$$

Here all quantities are calculated at the point $\boldsymbol{x}$, and the expression $F_0 = (2\pi)^{-1}\int_0^{2\pi} F\, d\theta$ should be determined separately for each form of the function F. In the case of the strain energy U, the adjoint structure is the same as the primary one. Moreover, assuming that $f = 0$ and $\boldsymbol{p}^0 = \boldsymbol{0}$ on the boundary Γ_ρ of a new hole, (2.21) becomes

$$\Im_G^D(\boldsymbol{x}) = \frac{h}{2E}[(\sigma_1 + \sigma_2)^2 + 2(\sigma_1 - \sigma_2)^2] \quad (2.22)$$

Now, let us consider the following functional of stresses and reactions

$$G = \int_\Omega H(\boldsymbol{\sigma})\, d\Omega + \int_{\Gamma_u} g(\boldsymbol{T})\, d\Gamma_u \quad (2.23)$$

where $H(\boldsymbol{\sigma})$ is the function of stresses $\boldsymbol{\sigma} = [\sigma_{11}, \sigma_{22}, \sigma_{12}]^{\top}$ and $g(\boldsymbol{T})$ denotes the function of reaction forces acting on the boundary Γ_u. In this case, the adjoint structure is of the form

$$
\begin{aligned}
\boldsymbol{\varepsilon}^{ai} &= \frac{\partial H}{\partial \boldsymbol{\sigma}} & \boldsymbol{p}^{a0} &= \boldsymbol{0} \quad \text{in } \Omega \\
\boldsymbol{T}^{a0} &= \boldsymbol{0} \quad \text{on } \Gamma_T & \boldsymbol{u}^{a0} &= -\frac{\partial g}{\partial \boldsymbol{T}} \quad \text{on } \Gamma_u
\end{aligned}
\tag{2.24}
$$

where $\boldsymbol{\varepsilon}^{ai}$ are the initial strains. The field of the initial strains induces a field of global strains in the form $\boldsymbol{\varepsilon}^a = \boldsymbol{\varepsilon}^{ai} + \boldsymbol{\varepsilon}^{ar}$, where $\boldsymbol{\varepsilon}^{ar}$ is the field of elastic strains. Now, in view of (2.24), the sensitivity of functional (2.23) with respect to introduction of a hole of an infinitesimally small radius ρ at the point $\boldsymbol{x}$, can be expressed analogously to (2.7), namely

$$
\delta G = \int_{\Omega} \boldsymbol{\varepsilon}^{ai} \delta \boldsymbol{\sigma} \, d\Omega - \int_{\Gamma_u} \boldsymbol{u}^{a0} \delta \boldsymbol{T} \, d\Gamma_u - \int_{\Gamma_\rho} H \, d\Gamma_\rho \delta \rho
\tag{2.25}
$$

where Γ_ρ denotes the boundary of this hole. Next, in view of the virtual work equation

$$
\int_{\Omega} \boldsymbol{\varepsilon}^{ar} \delta \boldsymbol{\sigma} \, d\Omega = \int_{\Omega} \boldsymbol{\sigma}^{ar} \delta \boldsymbol{\varepsilon} \, d\Omega = 0
\tag{2.26}
$$

and the complementary virtual work equation

$$
\int_{\Omega} \boldsymbol{\varepsilon}^{a} \delta \boldsymbol{\sigma} \, d\Omega = \int_{\Gamma_\rho} \boldsymbol{\sigma} \boldsymbol{\varepsilon}^a \, d\Gamma_\rho \delta \rho + \int_{\Gamma_u} \boldsymbol{u}^{a0} \delta \boldsymbol{T} \, d\Gamma_u - \int_{\Gamma_\rho} \boldsymbol{p}^0 \boldsymbol{u}^a \, d\Gamma_\rho \delta \rho
\tag{2.27}
$$

the first variation of functional (2.23) takes the form

$$
\delta G = \int_0^{2\pi} [(\boldsymbol{\sigma} \boldsymbol{\varepsilon}^a - H)h - \boldsymbol{p}^0 \boldsymbol{u}^a] \rho \, d\theta \delta \rho
\tag{2.28}
$$

It is easy to notice that for $\rho = 0$, the first derivative of the considered functional is equal zero. So, for $\rho = 0$, let us determine the second derivative of this functional. Then, we have

$$
\left. \frac{\partial^2 G}{\partial \rho^2} \right|_{\rho=0} = \lim_{\rho \to 0} \int_0^{2\pi} \left\{ \frac{\partial}{\partial \rho} [(\boldsymbol{\sigma} \boldsymbol{\varepsilon}^a - H)h - \boldsymbol{p}^0 \boldsymbol{u}^a] - \frac{\partial}{\partial \boldsymbol{n}} [(\boldsymbol{\sigma} \boldsymbol{\varepsilon}^a - H)h - \boldsymbol{p}^0 \boldsymbol{u}^a] + \right.
$$

$$
\left. + \frac{1}{\rho} [(\boldsymbol{\sigma} \boldsymbol{\varepsilon}^a - H)h - \boldsymbol{p}^0 \boldsymbol{u}^a] \right\} \rho \, d\theta
\tag{2.29}
$$

Analogously as in the case of functional (2.2), the first two terms on the right hand side of (2.29) cancel out and finally the topological derivative can be written as follows

$$\Im_G^D(\boldsymbol{x}) = h\left[\frac{1}{E}(\sigma_1 + \sigma_2)(\sigma_1^a + \sigma_2^a) + \frac{2}{E}(\sigma_1 - \sigma_2)(\sigma_1^a - \sigma_2^a)\cos 2\alpha - H_0\right] - \boldsymbol{p}^0\boldsymbol{u}^a$$
(2.30)

where

$$H_0 = \frac{1}{2\pi}\int\limits_0^{2\pi} H\, d\theta$$

2.2. Topological derivative for bending plates

Consider a plate occupying, referred to the middle surface, a domain $\Omega \subset R^2$, with a boundary Γ. The plate is subjected to the transverse load $\boldsymbol{p}^0$ in Ω, whereas either the generalized traction $\boldsymbol{T}^0$ or displacements are specified on Γ. Here, Kirchhoff's theory of thin plates is used, and the bending plate can be treated as a set of layers, each of which is in a plane state of stress.

Now, we confine our analysis to the case when the functional G is expressed by (2.2). Here, taking into account that $\boldsymbol{u} = [0,0,w]^\top$ on the middle surface, $f(\boldsymbol{u})$ can be interpreted as a function of transverse displacements w. Then, the topological derivative of the analyzed functional with respect to the introduction of an infinitesimally small, circular hole at the point $\boldsymbol{x} = (x_1, x_2)$ of the middle surface, can be determined analogously as in Section 2.1. So, in view of (2.21), we have

$$\Im_G^P(\boldsymbol{x}) = \int\limits_{-h/2}^{h/2}\left[\frac{1}{E}(\sigma_1 + \sigma_2)(\sigma_1^a + \sigma_2^a) + \frac{2}{E}(\sigma_1 - \sigma_2)(\sigma_1^a - \sigma_2^a)\cos 2\alpha - F_0\right]dx_3 - f - \boldsymbol{p}^0\boldsymbol{u}^a$$
(2.31)

where h denotes the thickness of the plate and x_3 is the coordinate normal to the middle surface. The principal stresses may be expressed as a function of x_3 in the form

$$\sigma_i(x_3) = 2\frac{\widehat{\sigma}_i}{h}x_3 \qquad\qquad \sigma_i^a(x_3) = 2\frac{\widehat{\sigma}_i^a}{h}x_3 \qquad\qquad i = 1,2 \qquad\qquad (2.32)$$

where $\widehat{\sigma}_i$, $\widehat{\sigma}_i^a$ are the principal stresses on the upper surface of the plate, respectively for the primary and adjoint structure. After substitution of (2.32) into (2.31) and integration, we have

$$\Im_G^P(\boldsymbol{x}) = \frac{h}{3E}[(\widehat{\sigma}_1 + \widehat{\sigma}_2)(\widehat{\sigma}_1^a + \widehat{\sigma}_2^a) + 2(\widehat{\sigma}_1 - \widehat{\sigma}_2)(\widehat{\sigma}_1^a - \widehat{\sigma}_2^a)\cos 2\alpha] +$$

$$\tag{2.33}$$

$$- \int_{-h/2}^{h/2} F_0\, dx_3 - f - \boldsymbol{p}^0\boldsymbol{u}^a$$

Taking into account that the principal moments in the primary and adjoint structure take the form

$$M_i = \int_{-h/2}^{h/2} \sigma_i x_3\, dx_3 \qquad M_i^a = \int_{-h/2}^{h/2} \sigma_i^a x_3\, dx_3 \qquad i = 1, 2 \qquad (2.34)$$

the topological derivative can be also presented as follows

$$\Im_G^P(\boldsymbol{x}) = \frac{12}{Eh^3}[(M_1 + M_2)(M_1^a + M_2^a) + 2(M_1 - M_2)(M_1^a - M_2^a)\cos 2\alpha] +$$

$$\tag{2.35}$$

$$- \int_{-h/2}^{h/2} F_0\, dx_3 - f - \boldsymbol{p}^0\boldsymbol{u}^a$$

When G coincides with the strain energy and assuming that $f = 0$ and $\boldsymbol{p}^0 = \boldsymbol{0}$ on the boundary Γ_ρ of a new hole, the topological derivative reduces to the form

$$\Im_G^P(\boldsymbol{x}) = \frac{h}{6E}[(\widehat{\sigma}_1 + \widehat{\sigma}_2)^2 + 2(\widehat{\sigma}_1 - \widehat{\sigma}_2)^2] \tag{2.36}$$

It can be also expressed by the principal moments, namely

$$\Im_G^P(\boldsymbol{x}) = \frac{6}{Eh^3}[(M_1 + M_2)^2 + 2(M_1 - M_2)^2] \tag{2.37}$$

Similar considerations can be performed as well for an arbitrary functional of stresses and reaction forces expressed by (2.23).

2.3. Topological derivative for cost functional

Next, let us consider the topological derivative of the global cost C. The cost of the structure, for example, can be assumed as proportional to the material volume. Then, it can be expressed as follows

$$C = c(V_0 - \pi\rho^2 h) \tag{2.38}$$

where c is a unit cost, V_0 denotes the initial volume of the considered structure, and, as previously, h denotes its thickness and ρ is the radius of the inserted small hole. Thus, the topological derivative of the cost functional with respect to the introduction of this infinitesimally small hole, takes the form

$$\Im_C(\boldsymbol{x}) = \frac{1}{2\pi} \frac{\partial^2 C}{\partial \rho^2}\bigg|_{\rho=0} = -ch \qquad (2.39)$$

3.   Optimal design method based on finite modification

In this section, conditions for the introduction of finite topology modification based on the topological derivative are derived. Also, sensitivity expressions with respect to the shape modification are presented. These conditions and formulas can be applied in order to formulate a heuristic algorithm for simultaneous topology and shape optimization.

3.1.   Conditions for introduction of finite topology modifications

We consider now a general optimization problem of the form

$$\min G \qquad \text{subject to} \quad C - C_0 \leqslant 0 \qquad (3.1)$$

where G is the objective functional (or function), C denotes the global cost (or global volume) and C_0 is the upper bound on the global cost. When G expresses the strain energy, the problem corresponds to maximization of the structure stiffness with the constraint set on the global cost.

At first, we take into account the optimal design with respect to dimensional and shape parameters s_i, $i = 1, 2, \ldots, n$. Using Lagrangian

$$L = G + \lambda(C - C_0) \qquad (3.2)$$

where λ ($\lambda \geqslant 0$) is the Lagrange multiplier, the optimality conditions take the form

$$\frac{\partial L}{\partial s_i} = \frac{\partial G}{\partial s_i} + \lambda \frac{\partial C}{\partial s_i} = 0 \qquad i = 1, 2, \ldots, n$$

$$\lambda(C - C_0) = 0 \qquad (3.3)$$

Therefore, the optimal values of design parameters s_i and Lagrange's multiplier λ can be determined in the incremental process of optimization.

Now, the condition of introduction of an infinitesimally small circular hole, using the concept of the topological derivative, takes the form

$$\Im(\boldsymbol{x}) = \Im_G(\boldsymbol{x}) + \lambda\Im_C(\boldsymbol{x}) < 0 \qquad (3.4)$$

where $\Im(\boldsymbol{x})$, $\Im_G(\boldsymbol{x})$, $\Im_C(\boldsymbol{x})$ are the topological derivatives at the point $\boldsymbol{x}$, respectively of the Lagrangian, objective functional G (in the case of plane elasticity problems it is denoted by $\Im_G^D(\boldsymbol{x})$, and in the case of plates – by $\Im_G^P(\boldsymbol{x})$) and cost functional C.

So, a new hole should be introduced at the point where the topological derivative of the Lagrangian $\Im(\boldsymbol{x})$ attains minimum and condition (3.4) is fulfilled. This approach is similar to the bubble method, however apart from the positioning of the hole it additionally formulates the condition of topology modification.
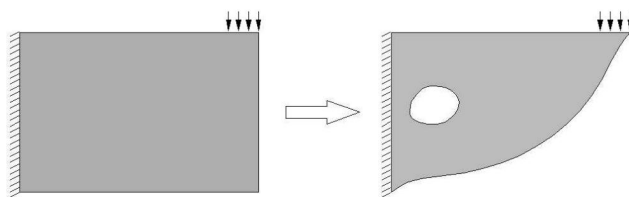
Fig. 1. Idea of simultaneous finite topology modification and shape optimization

The shape optimization of the new holes is a usually time-consuming and complicated process. In order to reduce these difficulties, a concept of finite modification is proposed (Fig. 1). We can distinguish two types of problems (cf. Bojczuk and Szteleblak, 2003, 2005). The first one corresponds to the introduction of holes of a prescribed size and shape. Assuming that, approximately, the introduction of a finite void can be treated as the inserting of a sum of infinitesimally small voids, the preliminary problem takes the form

$$\Delta L^{(opt)} = \min_{\boldsymbol{r}} \int\limits_{A_p} \Im(\boldsymbol{x})\, dA_p \qquad (3.5)$$

where A_p denotes a fixed area of the new hole and $\boldsymbol{r}$ is the vector of its position. The topology modification condition corresponds to negative value of this increment, namely

$$\Delta L^{(opt)} < 0 \qquad (3.6)$$

The second type of problems consists in the introduction of holes of an unknown size and shape together with the introduction of finite changes of

other boundaries. As for the redesign path related to the constant cost C_0 and minimum of the objective function G, the multiplier λ achieves its minimum at the optimal point, then for finite variations of design we can introduce the design quality function Λ (cf. Mróz and Bojczuk, 2003). Now, the preliminary problem takes the form

$$\min_A \Lambda \qquad \text{where} \qquad \Lambda = \frac{\mu\lambda + \Delta G}{\mu - \Delta C} = \frac{\mu\lambda + \int\limits_A \Im_G(\boldsymbol{x})\, dA}{\mu - \int\limits_A \Im_C(\boldsymbol{x})\, dA} \qquad (3.7)$$

Here, A denotes the unknown area of the hole and μ ($\mu \geqslant 0$) is the scaling factor. So, the condition of acceptance of the finite topology modification takes the form

$$\Lambda < \lambda \qquad (3.8)$$

When $\mu = 0$, problem (3.7) takes the form

$$\min_A \Lambda \qquad \text{where} \qquad \Lambda = -\frac{\Delta G}{\Delta C} = -\frac{\int\limits_A \Im_G(\boldsymbol{x})\, dA}{\int\limits_A \Im_C(\boldsymbol{x})\, dA} \qquad (3.9)$$

and the considered approach becomes analogous to the bubble method.

In order to solve problem (3.5) or (3.7) and check a proper condition for the introduction of finite topology modification, the finite element discretization is used. Then, the solution to the problem is relatively easy to obtain. However, it gives reduction of the structure cost, so in order to follow the path of the constant global cost we can, for example, apply the idea of proportional variation of thickness. The obtained design usually differs only a little from the global optimum.

3.2. Correction of structure shape

After the finite topology modification, only an improved structure is obtained, so an additional standard shape optimization should be performed. It can be done using optimality conditions (3.3) for optimization problem (3.1) with an updated vector of design parameters. When an arbitrary gradient method is used, we need sensitivity expressions with respect to the shape modification.

Now, we assume that shape variation of the domain Ω is given in the form of a transformation $f : \Omega \to \Omega^*$, namely

$$\boldsymbol{x}^* = \boldsymbol{x} + \delta\boldsymbol{\varphi} \qquad (3.10)$$

where $\boldsymbol{x}^*$ is the transformed position of the point $\boldsymbol{x}$ and, as previously, $\delta\boldsymbol{\varphi} = [\delta\varphi_1, \delta\varphi_2]^\top$ is variation of the shape transformation function. We also assume that the shape transformation of the boundary Γ_T is described by variation of the shape parameters a_l $(l = 1, 2, \ldots, L)$. Then, variation of the transformation function can be presented in the form

$$\delta\varphi_k = \sum_{l=1}^{L} \frac{\partial\varphi_k}{\partial a_l}\delta a_l \qquad k = 1, 2 \tag{3.11}$$

Now, let us consider particular cases of the shape transformation used in this paper. First, translation of a hole with a prescribed size and shape will be taken into account. Then, we have

$$\varphi_k = a_k \qquad k = 1, 2 \tag{3.12}$$

where a_1, a_2 are components of the translation vector $\boldsymbol{a}$. Finally, variation of the transformation function takes the form

$$\delta\varphi_1 = \delta a_1 \qquad \delta\varphi_2 = \delta a_2 \tag{3.13}$$

In order to provide a proper way of approximate boundary description, also with sharp edges, B-splines can be used (cf. Gerald and Wheatley, 1995; Kiciak, 2005). The recursive definition of the normalized B-spline function of the order k is

$$N_j^{(1)}(t) = \begin{cases} 1 & \text{for } t_j \leqslant t \leqslant t_{j+1} \\ 0 & \text{otherwise} \end{cases} \tag{3.14}$$

and

$$N_j^{(k)}(t) = \frac{t - t_j}{t_{j+k-1} - t_j}N_j^{(k-1)}(t) + \frac{t_{j+k} - t}{t_{j+k} - t_{j+1}}N_{j+1}^{(k-1)}(t) \tag{3.15}$$

where $\boldsymbol{t} = [t_1, t_2, \ldots, t_m]^\top$ is the knot vector created as a set of non-decreasing numbers. Now, a polynomial B-spline curve can be written as follows

$$\varphi_i(t) = \sum_{j=0}^{n} N_j^{(k)}(t)x_{i(j)} \qquad i = 1, 2 \tag{3.16}$$

where $\boldsymbol{x}_j = [x_{1(j)}, x_{2(j)}]^\top$ are coordinates of the jth control point.

The modification of the boundary can also be described by NURBS (non-uniform rational B-splines). In this case, we have (cf. Adamski, 1997; Kiciak, 2005)

$$\varphi_i(t) = \frac{\sum_{j=0}^{n} N_j^{(k)}(t)w_j x_{i(j)}}{\sum_{j=0}^{n} N_j^{(k)}(t)w_j} \qquad i = 1, 2 \tag{3.17}$$

where w_j is the weight of the point $\boldsymbol{x}_j$.

The possibility of control of the shape by only several control points and the possibility of local changes of shape without any influence on the rest of the structure are the main advantages of B-splines and NURBS. In this paper, B-splines of the order $k = 4$ (so-called cubic B-splines) are used. Here, in the shape optimization process, the coordinates of control points are the design variables. However, also the knot vector and weights of the control points can be used to modify the shape.

Now, let us consider sensitivity analysis of the functional of strains and displacements expressed by (2.2). Here, the adjoint structure specified by (2.4), (2.5) is introduced. Let us denote arbitrary shape parameters by a_l ($l = 1, 2, \ldots, L$). In the case of the considered here cubic B-splines, these parameters correspond to the coordinates of control points $x_{1(j)}$, $x_{2(j)}$, $j = 1, 2, \ldots, J$, $L = 2J$. Assuming that the conservative surface traction $\boldsymbol{T}^0$ is applied on Γ_T, the variation of functional (2.2) can be written in the form (cf. Dems, 1980; Kleiber, 1995)

$$
\delta G = \int\limits_{\Gamma_T} \sum_{k=1}^{2} \sum_{l=1}^{L} \Big[F - \boldsymbol{\sigma}^a \boldsymbol{\varepsilon} - 2(f + \boldsymbol{T}^0 \boldsymbol{u}^a) K + \frac{\partial}{\partial \boldsymbol{n}} (f + \boldsymbol{T}^0 \boldsymbol{u}^a) \Big] n_k \frac{\partial \varphi_k}{\partial a_l} \delta a_l \; d\Gamma_T +
$$
$$
\tag{3.18}
$$
$$
+ \int\limits_{\Omega} \overline{\delta \boldsymbol{p}}^0 \boldsymbol{u}^a \; d\Omega
$$

where, as previously, $\partial / \partial \boldsymbol{n}$ denotes a derivative in the direction normal to the modified boundary, K is the curvature of this boundary and $\overline{\delta \boldsymbol{p}}^0$ denotes local variation of volume forces referred to the initial shape.

Next, let us consider the functional of stresses and reaction forces expressed by (2.23). Here, adjoint structure (2.24) with initial strains and non-zero boundary conditions on Γ_u is introduced. Assuming the conservative surface traction $\boldsymbol{T}^0$ on Γ_T, the variation of functional (2.23) can be written in the form (cf. Dems, 1980; Kleiber, 1995)

$$
\delta G = \int\limits_{\Gamma_T} \sum_{k=1}^{2} \sum_{l=1}^{L} \Big[H - \boldsymbol{\sigma} \boldsymbol{\varepsilon}^a + \frac{\partial}{\partial \boldsymbol{n}} (\boldsymbol{T}^0 \boldsymbol{u}^a) - 2 \boldsymbol{T}^0 \boldsymbol{u}^a K \Big] n_k \frac{\partial \varphi_k}{\partial a_l} \delta a_l \; d\Gamma_T +
$$
$$
\tag{3.19}
$$
$$
+ \int\limits_{\Omega} \overline{\delta \boldsymbol{p}}^0 \boldsymbol{u}^a \; d\Omega
$$

For a particular case, when only the unloaded part Γ_0 of the boundary Γ_T can be modified and $f = 0$ on Γ_0, sensitivity expressions (3.18) and (3.19) take the simplified forms, namely

$$\delta G = \int\limits_{\Gamma_T} \sum_{k=1}^{2} \sum_{l=1}^{L} (F - \boldsymbol{\sigma}^a \boldsymbol{\varepsilon}) n_k \frac{\partial \varphi_k}{\partial a_l} \delta a_l \, d\Gamma_T \tag{3.20}$$

and

$$\delta G = \int\limits_{\Gamma_T} \sum_{k=1}^{2} \sum_{l=1}^{L} (H - \boldsymbol{\sigma} \boldsymbol{\varepsilon}^a) n_k \frac{\partial \varphi_k}{\partial a_l} \delta a_l \, d\Gamma_T \tag{3.21}$$

However, sensitivity expressions (3.18)-(3.21) are formulated for plane elasticity problems, analogously as in Section 2.2, they can be easily adapted to plate structures.

Moreover, let us consider the cost functional of the form

$$C = \int\limits_{V} c \, dV \tag{3.22}$$

where analogously to (2.38), c is a unit cost, and V denotes volume of the considered structure. Then, variation of this functional can be written as follows

$$\delta C = \int\limits_{\Gamma_T} \sum_{k=1}^{2} \sum_{l=1}^{L} c n_k \frac{\partial \varphi_k}{\partial a_l} \delta a_l \, d\Gamma_T \tag{3.23}$$

Presented here sensitivity expressions can be used in an arbitrary gradient method of shape optimization (shape correction).

4. Optimization algorithms and numerical examples

4.1. Optimal design by introduction of holes of prescribed size and shape

Let us assume that a hole (holes) with the prescribed shape and fixed area A_p should be introduced into a plane structure. Now, the problem of the form analogous to (3.1) is considered. It can be stated as a searching of such a position of the hole for which the functional expressed by (2.2) or (2.23) with constraints imposed on the global cost, attains minimum (maximum). Also, other constraints, for example geometrical constraints, can be additionally used. To solve the problem, a heuristic algorithm composed of two steps is proposed here.

In the first step, the hole is introduced in a place where the integral of the topological derivative over the domain of the hole is minimal (maximal).

So, in order to find the best position $\boldsymbol{r}$ of the hole, preliminary problem (3.5) should be solved.

In the second step, standard optimization procedures are employed to correct the position of the hole. When a gradient method is used, the sensitivity analysis with respect to horizontal and vertical translation of the hole is performed. Now, sensitivity expressions presented in Section 3.2 can be applied.

4.1.1. Example 1: Optimization of square hole position

Let us assume that for some technological reasons a square hole of dimensions $1\,\text{m}\times1\,\text{m}$ should be inserted into the rectangular domain $(4\,\text{m}\times6\,\text{m})$ of a plane structure (Fig. 2). This structure is made of steel (Young's modulus is $E = 2.1 \cdot 10^5\,\text{MPa}$ and Poisson's ratio $\nu = 0.3$). It is clamped on the lower edge, loaded by linearly distributed shear forces on the upper edge, and its initial thickness is $h = 30\,\text{mm}$ ($h = \text{const}$).
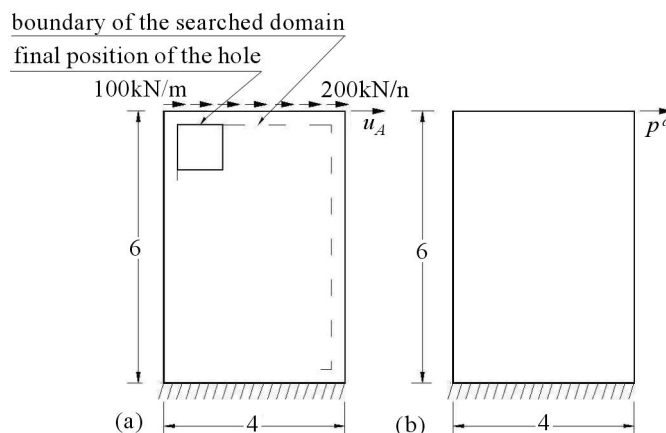
Fig. 2. Optimization of the position of a square hole (a) primary structure;
(b) adjoint structure

The optimization problem considered here is analogous to (3.1). The aim is to find the hole position which minimizes the horizontal displacement u_A of the point A with a condition imposed on the global cost proportional to the material volume. Also additional geometrical constrains, which assure that the hole lies inside the domain of the structure, are used here. A dashed line located $0.3\,\text{m}$ from the edges (Fig. 2a), denotes this admissible domain.

Now, the objective functional can be written in the form

$$G = \int_{\Gamma_T} \delta(\boldsymbol{x} - \boldsymbol{x}_A)u_1(\boldsymbol{x})\,d\Gamma_T = u_A \tag{4.1}$$

where $\delta(\boldsymbol{x} - \boldsymbol{x}_A)$ denotes Dirac's delta and $u_1(\boldsymbol{x})$ is the field of horizontal displacements. In order to solve the considered problem, an adjoint system of the same geometry and boundary conditions as the primary structure is introduced. Moreover, it is loaded at the point A by a unit force $P^a = 1$ acting in accordance with the direction of displacement u_A (Fig. 2b).

The optimal position of the hole, obtained directly after solution of preliminary problem (3.5), is shown in Fig. 2a. Now, both vertical and horizontal geometrical constraints are active, and correction of the hole position is not necessary. The ratio of the horizontal displacements u_A of the initial (without hole) and optimal design is $u_A^{(init)}/u_A^{(opt)} = 1.002$, and the final thickness arising from the cost (volume) condition equals $h = 31.304\,\text{mm}$. So, the introduction of the technological hole has not caused the effect of increase of the analyzed displacement and – on the contrary – even a small decrease has appeared here.

4.1.2. Example 2: Optimization of circular hole position

Let us assume that for technological reason a circular hole of 0.5 m diameter should be introduced into the rectangular plate (3 m×2 m) shown in Fig. 3. The structure is made of aluminium (Young's modulus is $E = 75\,\text{GPa}$ and Poisson's ratio $\nu = 0.35$). The initial thickness of the plate is 15 mm. The structure is clamped on three edges and the fourth (upper) edge is free (Fig. 3). The transverse load changes linearly along height of the plate.
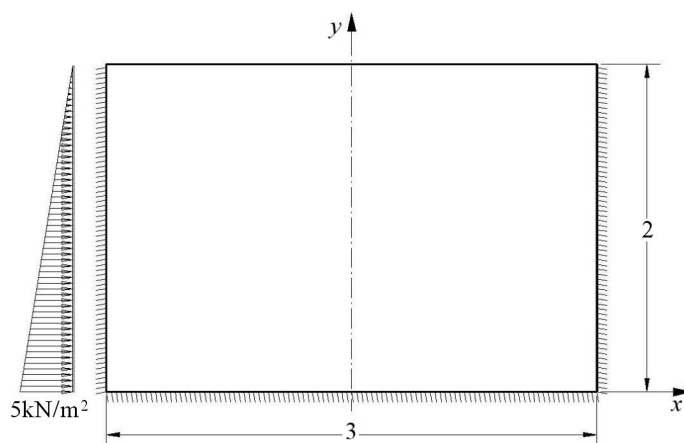
Fig. 3. Geometry of the plate

The aim of the optimization process is to find the hole position which minimizes the strain energy of the structure with a condition imposed on the

global cost proportional to the material volume. Additionally, geometric constraints, which assure that the hole lies inside the design domain, are used here. A dashed line situated 0.15 m from the edges (Fig. 4) denotes this admissible domain. Here, the objective functional, which expresses the strain energy, can be written in the form

$$G = \frac{1}{2} \int_\Omega \boldsymbol{M} \boldsymbol{\kappa} \, d\Omega \qquad (4.2)$$

where Ω is the middle surface of the plate, $\boldsymbol{M} = [M_1, M_2, M_{12}]^\top$ is the moment vector and $\boldsymbol{\kappa} = [\kappa_1, \kappa_2, \kappa_{12}]^\top$ denotes the curvature vector. Now, the adjoint structure is the same as the primary one. Two types of modification are analyzed here.
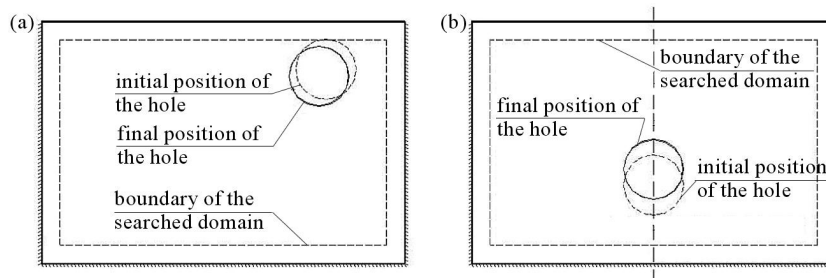
Fig. 4. Optimal position of the circular hole: (a) with unchanged load; (b) with removed load

In the first case, it is assumed that the overall load does not change. However, its part initially applied to the removed hole is replaced by the equivalent load distributed around it. It corresponds to the situation where the introduced hole is closed by a circular cover simply supported on the boundary. Now, in order to find the optimal position of the hole, at first preliminary problem (3.5) is solved, where the topological derivative expressed by (2.36) or (2.37) is used. The obtained design is presented in Fig. 4a by the dashed line. Next, correction of the hole position is performed. The optimal hole position is denoted by the continuous line, where coordinates of the hole center are $x_1^{(opt)} = 0.792$ m, $y_1^{(opt)} = 1.548$ m, and now geometrical constraints are not active. The ratio of the strain energy of the initial (without hole) and optimal design is $G^{(init)}/G^{(opt)} = 1.073$ and the final thickness arising from the cost condition equals $h = 15.507$ mm. Due to symmetry of the structure and loading, also the second, an equivalent solution with the symmetric position of the hole, namely $x_2^{(opt)} = -0.792$ m, $y_2^{(opt)} = 1.548$ m exists.

In the second case, it is assumed that the load is removed together with insertion of the hole. Now, the topological derivative expressed by (2.36) or

(2.37) should be completed by an additional term, namely $(-\boldsymbol{p}^0\boldsymbol{u})$. Then, solving preliminary problem (3.5), we get the initial position of the hole, which is presented in Fig. 4b by the dashed line. The optimal position of the hole, denoted by the continuous line, is obtained by standard optimization. The coordinates of the hole center, which lies on the symmetry axis, are $x_3^{(opt)} = 0.000\,\mathrm{m}$, $y_3^{(opt)} = 0.785\,\mathrm{m}$, and the ratio of the strain energy of the initial and optimal design is $G^{(init)}/G^{(opt)} = 1.274$.

4.2. Optimal design by introduction of finite topology and shape modifications

Let us consider the optimization problem of form (3.1). Here, it can be treated as the search for such a size and shape of a hole (holes) and shape of variable boundaries for which the functional expressed by (2.2) or (2.23) with constraints imposed on the global cost attains minimum (maximum). Also, other constraints, for example geometrical constraints, can be additionally used. In order to solve the problem, a heuristic algorithm for simultaneous topology and shape optimization composed of two mutually interacted stages is proposed here.
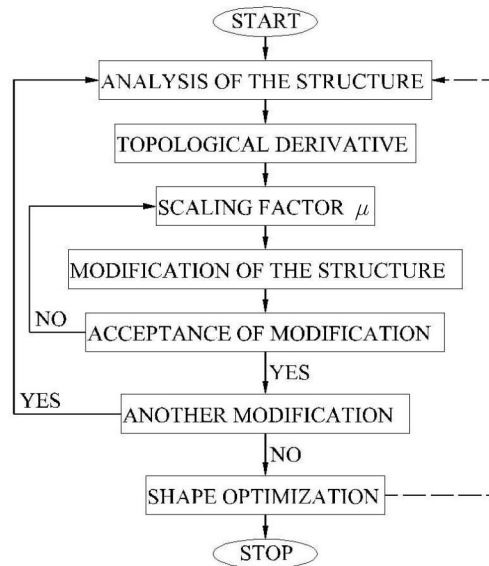
Fig. 5. Flowchart of the optimization process by finite topology and shape modification

At the first stage, the finite modification by introduction of a hole or change of a variable boundary is applied. In order to choose the best modification, the

preliminary problem of form (3.7) should be solved. Quantity of the removed boundary is controlled by the parameter μ ($\mu \geqslant 0$). When the objective functional after finite modification does not decrease, the value of the coefficient μ can be reduced. This procedure is repeated until it is possible to introduce any finite modification.

At the second stage, standard shape optimization procedures are used to smooth the variable boundaries. The boundaries of new holes are described by some additional shape parameters. So, the problem of form analogous to (3.1), but with an updated vector of design variables should be solved. It can be done using an arbitrary gradient method where optimality conditions are expressed by (3.3) and respective sensitivity formulas are presented in (3.18)-(3.21) and (3.23). Next, especially when huge changes are inserted during the shape optimization process, we can return to the first stage.

When any modification is not possible to introduce, the process of simultaneous topology and shape optimization is finished. A general flowchart of the optimization process is shown in Fig. 5.

4.2.1. *Example 3: Optimization of topology and shape of plane bridge structure*

Let us consider optimal design problem (3.1) for a plane structure shown in Fig. 6a, where G corresponds to the strain energy U and the cost C is proportional to the material volume. Also additional geometrical constraints are used here, namely it is assumed that the domain above the dashed line can not be removed.
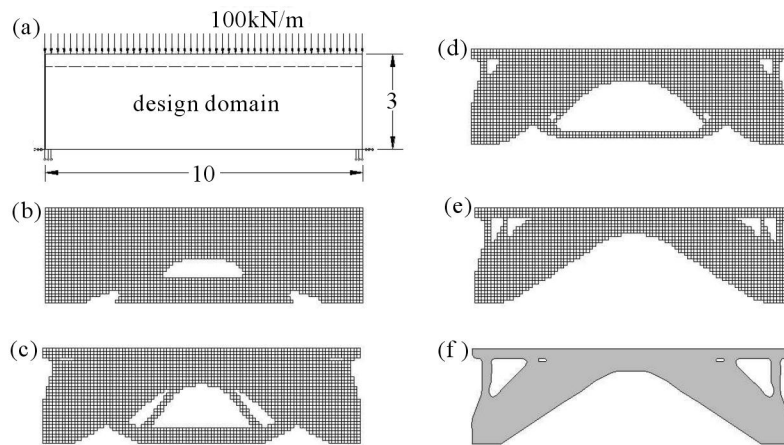
Fig. 6. Optimal design of the bridge structure ($\mu = 0.6$): (a) initial structure;
(b)-(e) every fifth successive finite modification; (f) final design

The structure is simply supported on a part of the lower edge and loaded by vertical forces on the upper edge. It is assumed that it has a constant thickness in the whole domain, which can change during the optimization process. The material properties are as follows: Young's modulus $E = 1.5 \cdot 10^4$ MPa, Poisson's ratio $\nu = 0.167$. The structure is divided into 3000 finite elements. Two cases are considered here.

In the first case, the scaling factor $\mu = 0.6$ is assumed. The history of optimization is shown in Fig. 6. The optimal structure (Fig. 6f) is obtained after 18 finite modifications and final shape optimization. The ratio of the strain energies of the initial and optimal design is $U^{(init)}/U^{(opt)} = 1.406$.

In the second case, the scaling factor $\mu = 3.0$ is assumed. The process of optimization is shown in Fig. 7, and now the optimal structure (Fig. 7e) is obtained only after 7 finite modifications and final shape optimization. The ratio of the strain energies of the initial and optimal design is $U^{(init)}/U^{(opt)} = 1.456$.
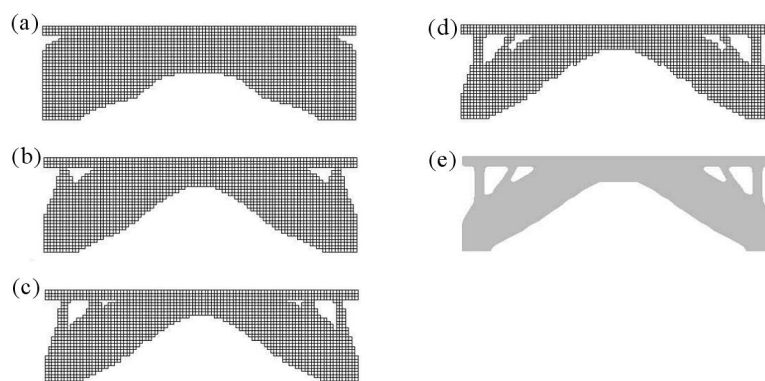
Fig. 7. Optimal design of the bridge structure ($\mu = 3.0$): (a) initial structure; (b)-(e) every second successive finite modification; (f) final design

It is important to notice that the assumption of a bigger value of the scaling factor μ accelerates the optimization process. However, when a too large value of μ is taken, it may lead to some difficulties – for example to the loss of structure connectivity. The coefficient μ should be chosen and modified by the user. Moreover, the optimal solution is not unique (compare Fig. 6f and Fig. 7e), and we may expect local optima.

4.2.2. Example 4: Optimization of topology and shape of plane, beam-like structure

The next application is the optimal design of a plane, beam-like structure shown in Fig. 8a. The optimization problem is the same as in the previous

example, i.e. to minimize the strain energy with a condition imposed on the cost, where the cost is proportional to the material volume. The structure is made of steel with Young's modulus $E = 2.1 \cdot 10^5$ MPa and Poisson's ratio $\nu = 0.3$. It is divided into 2880 finite elements.
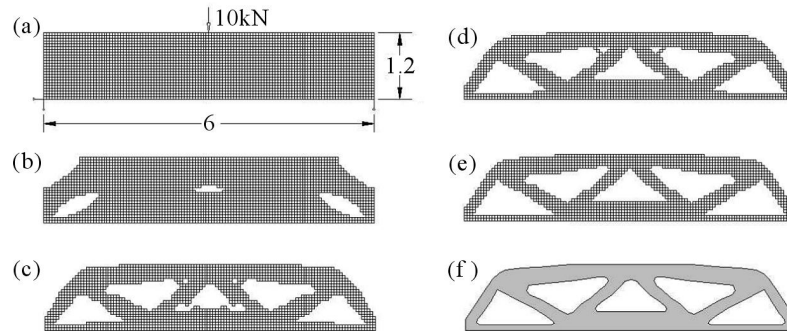
Fig. 8. History of optimization: (a) initial structure; (b)-(e) successive finite modifications; (f) final design

The history of optimization is shown in Fig. 8. The optimal structure, presented in Fig. 8f, is obtained after 5 finite modifications and final correction of the shape. The ratio of the strain energies of the initial and optimal design is $U^{(init)}/U^{(opt)} = 1.275$.

4.2.3. Example 5: Optimization of topology and shape of simply supported plate

The rectangular plate ($200\,\text{mm} \times 100\,\text{mm}$) shown in Fig. 9 is analyzed. The structure is made of steel. It is simply supported on each edge and loaded by a uniformly distributed load, non-symmetrically located near the center of the structure. The initial thickness of the plate is 5 mm.
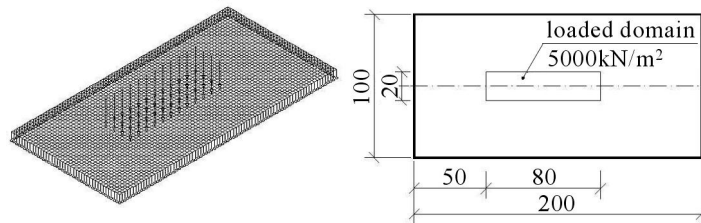
Fig. 9. Geometry of the plate, boundary and loading conditions

Now, let us consider again optimal design problem (3.1). Here G corresponds to the strain energy U and the cost C is proportional to the material volume. The maximum value of the plate thickness is limited to 20 mm.
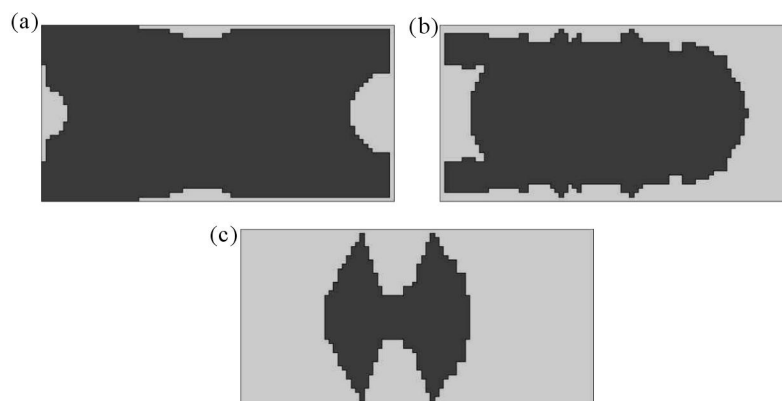
Fig. 10. History of optimization: (a)-(c) every second iteration of thickness reduction
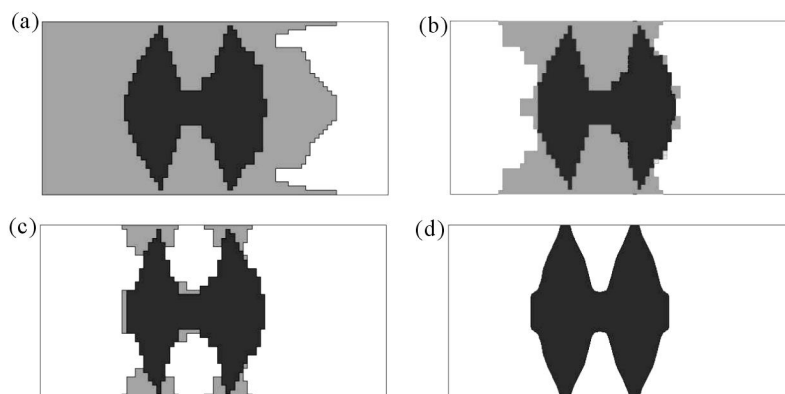
Fig. 11. History of optimization: (a)-(c) every second iteration of middle layer
removal; (d) final design obtained after shape correction

When, in the optimization procedure the material is removed all along the
thickness of the plate, often non-connectivity of the structure appears. This
situation, for example, takes place near simply supported edges. In order to
avoid these difficulties, the process of material removal is divided into two
phases. In the first phase, using condition (3.7) based on the topological deri-
vative, the thickness of the plate is symmetrically reduced by 2/3, see Fig. 10,
where the lighter colour denotes the smaller thickness. It is a pre-selection of
the domain, which may be completely removed. In the second phase, using
condition analogous to (3.7), but based on the shear energy, only the material
from the thin layer is successively reduced (Fig. 11a,b,c). Next, the thickness of
the non-removed domain is equalized. Finally, shape optimization is performed
and the optimal structure is shown in Fig. 11d. Constraints imposed on thick-

ness of the structure are active. During the optimization process, the strain energy was reduced from 2.107 J down to 0.0811 J ($U^{(init)}/U^{(opt)} = 26.292$).

4.2.4. Example 6: Optimization of topology and shape of clamped plate

Let us consider optimal design problem (3.1) for a plate structure shown in Fig. 12. As previously, G corresponds to the strain energy U and the cost C is proportional to the volume of the structure. It is assumed that areas bounded by the broken line and denoted as the "passive domain" can not be removed. Moreover, a condition on the maximal thickness of the plate is imposed.
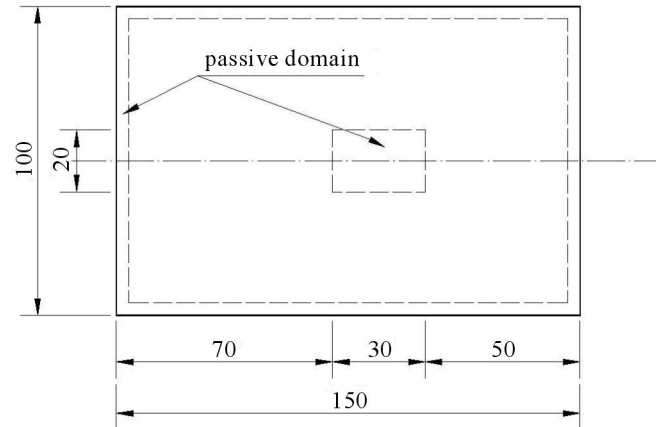
Fig. 12. Geometry of the plate

The rectangular plate ($150\,\text{mm} \times 100\,\text{mm}$) is made of aluminium with Young's modulus is $E = 75\,\text{GPa}$ and Poisson's ratio $\nu = 0.35$. Its initial and maximal thicknesses are respectively $5\,\text{mm}$ and $15\,\text{mm}$. The structure is uniformly loaded on all edges of the external rectangle by transverse forces of intensity $q = 5\,\text{kN/m}$. The plate is clamped along the non-symmetrically located internal rectangle, marked by the broken line in Fig. 12.

Here, analogously as in the previous example, the process of material removal is divided into two phases. In the first phase, thickness of the plate is symmetrically reduced by 2/3. Figure 13 illustrates this step, where the darker colour denotes the total thickness. In the second phase, the material from the central layer is successively reduced (Fig. 14a,b,c). Next, shape optimization of the structure with equalized thickness is performed. The optimal structure is shown in Fig. 14d. The constraints imposed on the maximum thickness of the structure are active. The rtio of strain energies before and after optimization is $U^{(init)}/U^{(opt)} = 6.585$.
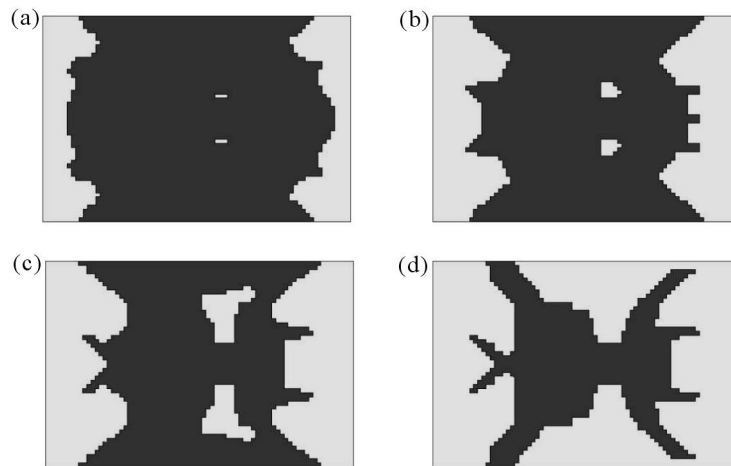
Fig. 13. History of optimization: (a)-(d) every second iteration of thickness reduction
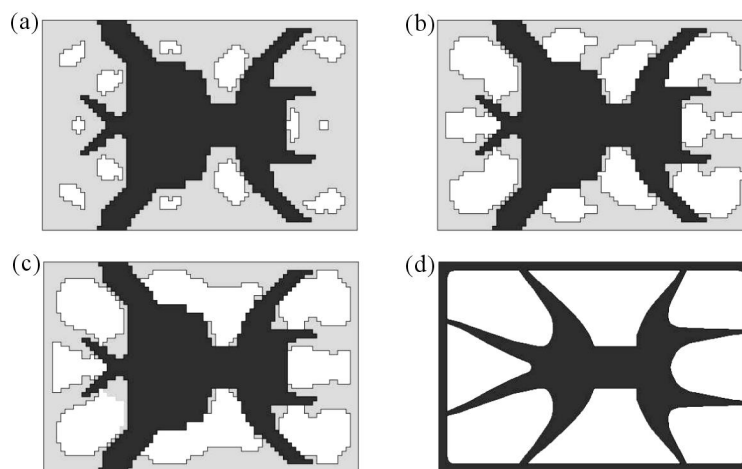
Fig. 14. History of optimization: (a)-(c) every second iteration of thin layer removal; (d) optimal design obtained after shape correction

5. Concluding remarks

A heuristic algorithm of simultaneous topology and shape optimization which uses finite topology modifications is presented in the paper. It is applied to optimal design of 2D structures working in a plane state of stress and being Kirchhoff's plates. It is important to notice that the application of finite modifications essentially reduces computation time required for generation of

improved or optimal designs. Another advantage of this method arises from the natural way of evolution of the optimal design. Here, the optimization process can be stopped at any level of the structure complexity, and usually the objective functional only slightly differs from the global minimum.

Numerical examples shown in the paper confirm the applicability and usefulness of the approach.

References

1. Adamski W., 1997, Application of NURBS in numerical modeling of objects, *Proceedings of the XIII Polish Conference on Computer Methods in Mechanics*, Garstecki A., Rakowski J. (edit.), Politechnika Poznańska, **1**, 89-97

2. Bojczuk D., Szteleblak W., 2003, Design optimisation for plane elasticity problems using finite topology variations, *Proceedings of the 15th International Conference on Computer Methods in Mechanics*, Wisła, CD ROM

3. Bojczuk D., Szteleblak W., 2005, Topology and shape optimization of plates using finite variations, *Proceedings of the 16th International Conference on Computer Methods in Mechanics*, Częstochowa, CD ROM

4. Burczyński T. (edit.), 2002, Computational sensitivity analysis and evolutionary optimization of systems with geometrical singularities, *Zeszyty Naukowe Katedry Wytrzymałości Materiałów i Metod Komputerowych Mechaniki*, Politechnika Śląska, Gliwice

5. Burczyński T., Kokot G., 2003, Evolutionary algorithms and boundary element method in generalized shape optimization, *J. Theor. and Appl. Mech.*, **41**, 2, 341-364

6. Czarnecki S., Dzierżanowski G., Lewiński T., 2004, Topology optimization of two-component plates, shells and 3D bodies, *Optimal shape design and modelling, Selected papers presented at WISDOM 2004*, Lewiński T., Sigmund O., Sokołowski J., Żochowski A. (edit.), Akademicka Oficyna Wydawnicza EXIT, Warszawa, 15-29

7. Dems K., 1980, Wieloparametrowa optymalizacja kształtu konstrukcji, *Zeszyty Naukowe*, **371**, Politechnika Łódzka, Łódź

8. Eschenauer H.A., Kobelev V.V., Schumacher A., 1994, Bubble method for topology and shape optimization, *Struct. Optim.*, **8**, 42-51

9. GERALD C.F., WHEATLEY P.O., 1995, *Applied Numerical Analysis*, Addison-Wesley Publishing Company

10. IL'IN A.M., 1992, Matching of asymptotic expansions of solutions of boundary value problems, *Translations of Mathematical Monographs*, **102**, AMS

11. KICIAK P., 2005, *Podstawy modelowania krzywych i powierzchni*, WNT, Warszawa

12. KLEIBER M. (EDIT.), 1995, *Komputerowe metody mechaniki ciała stałego*, PWN, Warszawa

13. MARCZEWSKA I., SOSNOWSKI W., MARCZEWSKI A., BEDNAREK T., 2003, Topology and sensitivity – based optimization of stiffened plates and shells, *Short Papers of the Fifth World Congress of Structural and Multidisciplinary Optimization*, 271-272

14. MRÓZ Z., BOJCZUK D., 2003, Finite topology variations in optimal design of structures, *Struct. Multidisc. Optim.*, **25**, 153-173

15. SOKOŁOWSKI J., ŻOCHOWSKI A., 1999, On topological derivative in shape optimization, *SIAM J. Control and Optimiz.*, **37**, 4, 1251-1272

**Zastosowanie modyfikacji skończonych w optymalizacji topologii
i kształtu konstrukcji dwuwymiarowych**

Streszczenie

W pracy rozpatrywana jest metoda jednoczesnej optymalizacji topologii i kształtu konstrukcji dwuwymiarowych przy użyciu skończonych modyfikacji topologii. Rozważania dotyczą zarówno konstrukcji tarczowych pracujących w płaskim stanie naprężenia, jak i płyt Kirchhoffa pracujących w stanie zgięciowym. Przy wykorzystaniu pochodnej topologicznej wyprowadzono warunki wprowadzania skończonych modyfikacji topologii. Gdy spełniony jest odpowiedni warunek modyfikacji, do konstrukcji wprowadzane są otwory o skończonych wymiarach oraz ewentualnie skończone modyfikacje pozostałych brzegów. Następnie wykonywana jest standardowa optymalizacja kształtu otworów i brzegów zewnętrznych. Analizowane są dwa podstawowe typy modyfikacji, a mianowicie wprowadzanie otworów o zadanej wielkości i kształcie oraz wprowadzanie otworów o nieznanej wielkości i kształcie wraz z ewentualną skończoną zmianą pozostałych brzegów. W pracy sformułowano odpowiedni algorytm heurystyczny optymalizacji topologii i kształtu rozpatrywanych konstrukcji. Przedstawione przykłady ilustracyjne potwierdzają przydatność zaproponowanego podejścia.